

**Speed-of-Sound Measurements Using Spherical Resonator
and Acoustic Virial Coefficients for Gaseous 1,1,1-Trifluoroethane (R-143a)¹**

Kazuhiro Ogawa,² Takeshi Kojima,^{2,3} and Haruki Sato²

-
1. Paper to be presented at the Fourteenth Symposium on Thermophysical Properties, June, 25-30, 2000.
 2. Department of System Design Engineering, Faculty of Science and Technology
Keio University, 3-14-1, Hiyoshi, Kohoku-ku, Yokohama, 223-8522, Japan.
 3. To whom correspondence should be addressed.

Abstract

The speed-of-sound measurement with a spherical resonator is recognized as one of the most precise and reliable approach to determine the ideal-gas heat-capacities and to reveal the thermodynamic properties of rarefied gases. In this study, we applied a spherical resonator to measure the speed-of-sound in gaseous 1,1,1-trifluoroethane, R-143a.

Seventy speed-of-sound values were obtained along five isotherms from 303 K to 343 K and up to 500 kPa in pressure. In addition, c_p^0 values and acoustic second virial coefficients were determined at each temperature of isotherm. Sample purity was 99.95 area% analyzed by the manufacturer. The experimental uncertainties based on the ISO Guide (1993) are estimated ± 8 mK in temperature, ± 0.2 kPa in pressure and ± 72 ppm in speed of sound with a coverage factor of $k=2$.

We compared the c_p^0 values determined from the measurements with those from theoretical calculation and confirmed the agreement between them within ± 0.1 %. Although any impurity component is still missing in the previous sample fluid, it is clear that the sample fluid effected to the systematic error in the previous results. New reliable speed-of-sound measurements, c_p^0 , and acoustic second virial coefficients of R-143a are presented in this paper.

Key word: 1,1,1-trifluoroethane, acoustic virial coefficient, alternative refrigerant, ideal-gas heat-capacity, R-143a, second virial coefficient, speed-of-sound, spherical resonator, virial equation of state

Introduction

The speed-of-sound values in gaseous HFC refrigerants: not only pure refrigerants of R-32, R-152a, R-143a, R-134a, and R-125, but also binary and ternary refrigerants of R-32/134a, R-32/125, R-32/125/134a, have measured using a spherical resonator in our group.^{1,2,3,4,5,6,7} The ideal-gas heat-capacities c_p^0 are determined from the measurements for pure refrigerants. On the other hand, the c_p^0 values can be determined from theoretical approach based on spectroscopic data. The theoretical c_p^0 values of six HFC refrigerants are also reported in our group by Yokozeki *et al.*⁸ Except for R-143a, the c_p^0 values of HFC refrigerants determined from the measurements satisfactorily agree with those from theoretical approach within respective uncertainties. Regarding R-143a we re-measured the speed of sound using different sample fluid from that of previous measurement. The ideal-gas heat-capacity and the acoustic second virial coefficient \bullet_a are newly determined from the speed-of-sound measurements.

Experimental Procedure

An explanation of the data acquisition processing for the present measurements was reported in Ref. 2. As illustrated in Figure 1, the sample gas was introduced into a pressure vessel Q from a supply bottle O. The inside and outside of the spherical resonator S were filled with the sample gas. After confirming a stable thermodynamic equilibrium condition in terms of the temperature T being within ± 0.1 mK and the pressure P within ± 0.01 kPa, the frequency, amplitude, and phase difference were measured at the condition of radially symmetric-mode resonance of the sample gas in the spherical resonator. The speed of sound, W , was then determined from the values of resonance frequency, $f_{l,n}$, and half-width, $g_{l,n}$, which were calculated from the measured

values of the frequency, amplitude, and phase difference. The relation among W , $f_{l,n}$ and $g_{l,n}$ is given by a complex expression as the same expression reported by Moldover *et al.*⁹,

$$f_{l,n} - ig_{l,n} = \frac{W \cdot Z_{l,n}}{2\pi a} + \sum_j (\Delta f - i\Delta g)_j \quad (1)$$

$$(l=0, 1, 2, \dots; n=0, 1, 2, \dots)$$

where a and $Z_{l,n}$ in the first term on the right-hand side are the radius of spherical resonator about 50 mm and n -th root of l -th order Bessel function, respectively. A certain mode is expressed by (l, n) , where the $l=0$ denotes radially symmetric mode. The second term on the right-hand side is a series of perturbation terms to represent various non-ideal conditions. Four radially symmetric modes, $(0, 2)$ through $(0, 5)$, are used in the present data processing. When a series of measurements was completed at certain state point, we reduce the pressure step by step under the isothermal condition for succeeding measurements at lower pressure.

Result and Discussion

The expanded uncertainties based on the ISO Guide (1993) in temperature, pressure, and speed-of-sound measurements are estimated to be ± 8.0 mK, ± 0.2 kPa, and ± 72 ppm, respectively. The coverage factor, k , is adopted as being 2.

The purity of sample purified and analyzed by the manufacturer was better than 99.95 % in the gas-chromatograph area fraction for R-143a. No further purification except degasing was applied in the present study.

Seventy speed-of-sound values in gaseous R-143a were measured along five isotherms, 303, 313, 323, 333, and 343 K, and at pressures from 10 to 500 kPa, which are summarized in Table 1. The present results are the average values of the

measurements at four different radially symmetric resonance modes from (0, 2) to (0, 5). The thermophysical property values used in the perturbation terms of eq. (1) for the correction to the present measurements are the ideal-gas heat-capacity¹⁰, the equation of state¹¹, the thermal conductivity¹², and the viscosity values estimated from the modified Eucken equation¹². A contribution of the perturbation terms is estimated being an order of magnitude of 100 ppm to speed-of-sound values and the uncertainty due to these corrections is 10 ppm for the speed-of-sound values.

The squared measured speed-of-sound data were correlated along each isotherm with the following quadratic function of pressure,

$$W^2 = \frac{\tilde{a}^0 RT}{M} \left\{ 1 + \tilde{a}_a \left(\frac{p}{RT} \right) + \tilde{a}_a \left(\frac{p}{RT} \right)^2 \right\} \quad (2)$$

where superscript naught denotes the ideal-gas condition; R is molar gas constant; M is the molar mass; β_a and γ_a are the second and third acoustic-virial coefficients; and γ is the specific-heat ratio. We used the molar gas constant, 8.314472 J mol⁻¹K⁻¹, which was determined from the similar acoustic method by Moldover *et al.*¹³ and corrected for the International Temperature Scale of 1990.¹⁴

Figure 2 shows the present speed-of-sound measurements on a speed-of-sound pressure diagram. The speed of sound differential with respect to the pressure along each isotherm becomes slightly negative.

Figure 3 shows the deviation of the speed-of-sound measurements at four different radially symmetric modes from (0, 2) to (0, 5), from eq. (2) at 303.143 K. All measurements are well represented by eq. (2) within the estimated uncertainty of 72 ppm.

The ideal-gas heat-capacity, c_p^0 , the second, and third acoustic virial

coefficient, β_a , γ_a , determined from the speed-of-sound measurements, are summarized in Table 2 and Table 3. The c_p^0 , β_a , and γ_a , were simply determined from eq. (2) at each temperature. The maximum standard deviations due to the fitting to the squared speed-of-sound measurements by eq. (2) for c_p^0 , β_a , and γ_a were 0.033 %, 0.14 %, and 16 %, respectively.

We compared the c_p^0 values determined from the speed-of-sound measurements with those from theoretical calculation and confirmed the agreement between them within ± 0.1 % as shown in Fig. 4 for R-143a. It should be noticed that the c_p^0 values for R-143a was measured after the calculation by Yokozeki *et al.*

Conclusions

We measured 70 speed-of sound values for R-143a in the gaseous phase. The values of c_p^0 , β_a , and γ_a , were derived from the speed-of-sound measurements. The c_p^0 values determined from our measurements in gaseous R-143a agree with those from theoretical approach within ± 0.1 %.

Acknowledgments

The authors thank the New Energy and Industrial Technology Development Organization, Tokyo, for the financial support of the present study.

Literature Cited

1. Hozumi, T.; Sato, H.; and Watanabe, K. *J. Chem. Eng. Data* **1994**, 39, 3, 493.
2. Hozumi, T.; Koga, T.; Sato, H.; and Watanabe, K. *Int. J. Thermophys.* **1993**, 14, 4, 739; Erratum, *Int. J. Thermophys.* **1994**, 15, 2, 385.
3. Hozumi, T.; Sato, H.; and Watanabe, K. *J. Chem. Eng. Data* **1996**, 41, 5, 1187.
4. Hozumi, T.; Sato, H.; and Watanabe, K. *Int. J. Thermophys.* **1995**, 17, 3, 587.
5. Ichikawa, T.; Ogawa, K.; Sato, H.; Watanabe, K. *Proc. of the 5th Asian Thermophys. Prop. Conf.* **1998**, 535.
6. Ichikawa, T.; Hozumi, T.; Sato, H.; Watanabe, K. *Abst. of the 13th Symp. on Thermophys. Prop.* **1997**, 45.
7. Hozumi, T.; Sato, H.; Watanabe, K. *J. Chem. Eng. Data* **1997**, 42, 3, 541.
8. Yokozeki, A.; Sato, H.; Watanabe, K. *Int. J. of Thermophys.* **1998**, 19, 1, 89.
9. Moldover, M. R.; Trusler, J. P. M.; Edwards, Y. J.; Mehl, J. B.; Davis, R. S. *J. Res. Nat. Bur. Stand.* **1988**, 93, 2, 85.
10. Gillis, K. A. *Int. J. Thermophys.* **1997**, 18, 1, 73.
11. Hozumi, T.; Sato, H.; Watanabe, K. private communication, the virial equation of state for R-143a were developed by the $p \cdot T$ values of de Vries¹⁶ and Zhang *et al.*¹⁷
12. Reid, T. C.; Prausnitz, J. M.; Poling, B. E. *The Properties of Gases & Liquids*, 4th ed. McGraw-Hill, New York, **1987**, 401-403, 493.
13. Moldover, M. R.; Boyes, S. J.; Meyer, C. W.; Goodwin, A. H. R. *J. Res. Nat. Ins. Stand. Tech.* **1999**, 104, 1, 11.
14. Preston-Thomas, H. *Metrologia* **1990**, 27, 3.
15. Beckermann, W.; Kohler, F. *Int. J. Thermophys.* **1995**, 16, 2, 455.

16. TRC Thermodynamic Tables, Non-Hydrofluorocarbons, Texas A&M University:
College Station, TX, USA, **1989**, IX, v-6881.
17. deVries, B. DKV, No. 55, Forch.-Ber., DKV-Verlag, Germany **1997**.
18. Zhang, H. -L.; Sato, H.; Watanabe, K. *J. Chem. Eng. Data* **1995**, 40, 4, 887.

Table 1. Speed of sound for R-143a

T / K	p / kPa	$W / \text{m}\cdot\text{s}^{-1}$	T / K	p / kPa	$W / \text{m}\cdot\text{s}^{-1}$
303.143	505.52	171.282	323.133	497.43	179.103
303.143	401.15	173.862	323.133	401.00	181.010
303.143	300.90	176.266	323.133	300.95	182.950
303.143	200.78	178.599	323.133	201.12	184.849
303.143	180.54	179.064	323.133	180.84	185.231
303.143	160.74	179.516	323.133	160.67	185.610
303.143	140.68	179.971	323.133	140.84	185.979
303.143	120.75	180.420	323.133	120.65	186.355
303.143	100.76	180.869	323.133	100.78	186.723
303.143	80.80	181.315	323.133	80.54	187.096
303.143	60.80	181.760	323.133	60.69	187.462
303.143	40.77	182.203	323.133	40.56	187.832
303.143	20.70	182.645	323.133	20.59	188.198
303.143	10.74	182.868	323.133	10.65	188.380
313.144	508.06	175.148	333.141	501.45	182.583
313.144	401.18	177.508	333.141	401.20	184.371
313.144	300.71	179.668	333.141	301.04	186.130
313.144	200.95	181.762	333.141	200.79	187.862
313.144	180.66	182.184	333.141	180.66	188.208
313.144	160.86	182.593	333.141	160.80	188.548
313.144	140.68	183.008	333.141	140.38	188.896
313.144	120.84	183.414	333.141	120.76	189.229
313.144	100.69	183.824	333.141	100.77	189.568
313.144	80.77	184.228	333.141	80.69	189.907
313.144	60.62	184.635	333.141	60.76	190.243
313.144	40.73	185.035	333.141	40.70	190.580
313.144	20.72	185.437	333.141	20.51	190.920
313.144	10.69	185.638	333.141	10.64	191.087

T / K	p / kPa	$W / \text{m}\cdot\text{s}^{-1}$
343.142	502.43	185.977
343.142	401.19	187.615
343.142	301.10	189.214
343.142	200.91	190.793
343.142	180.87	191.108
343.142	159.76	191.437
343.142	140.75	191.734
343.142	120.81	192.043
343.142	100.82	192.353
343.142	80.64	192.665
343.142	60.69	192.973
343.142	40.43	193.286
343.142	20.73	193.592
343.142	10.73	193.747
*343.141	501.43	185.937
343.141	400.82	187.566
343.141	300.72	189.168
343.141	200.87	190.745
343.141	180.81	191.059
343.141	160.86	191.371
343.141	140.76	191.685
343.141	120.24	192.004
343.141	100.73	192.306
343.141	80.77	192.616
343.141	60.70	192.926
343.141	40.75	193.235
343.141	20.44	193.549
343.141	11.90	193.687

*, previous sample.

Table 2. c_p^0 for R-143a

T / K	c_p^0 / R	uncertainty due to the fitting, %
303.143	9.487	0.033
313.144	9.704	0.028
323.133	9.903	0.025
333.141	10.098	0.025
343.142	10.295	0.029

Table 3. β_a , and γ_a for R-143a

T / K	$\beta_a / \text{cm}^3 \cdot \text{mol}^{-1}$	uncertainty due to the fitting, %	$\gamma_a / \text{dm}^6 \cdot \text{mol}^{-2}$	uncertainty due to the fitting, %
303.143	-600.5	0.13	-0.111	3.4
313.144	-557.0	0.10	-0.082	3.5
323.133	-517.8	0.08	-0.059	3.5
333.141	-483.5	0.09	-0.036	6.6
343.142	-451.1	0.14	-0.022	16

Figure Captions

Figure 1. Experimental apparatus: (A) PID controller; (B) Thyristor regulator; (C) Transformer; (D1, D2) Thermometer bridges; (E1, E2) Platinum resistance thermometers; (F) Refrigeration units; (G) Stirrer; (H1, H2) Heaters; (I) Voltmeter; (J) Frequency synthesizer; (K) Lock-in amplifier; (L) Pressure gage; (M1)(M2) Transducers; (N) Vacuum pump; (O) Supply bottle; (Q) Pressure vessel; (R) Expansion bottle; (S) Spherical resonator; (T) Recovering bottle; (U) Thermostated bath; (V) Valves.

Figure 2. Speed-of-sound measurements for R-143a: ●, 303K; ■, 313K; •, 323K; ▲, 333K; ◇, 343 K; ×, 343 K (previous sample).

Figure 3. Difference among the speed-of-sound values at different modes: ●, (0, 2); ■, (0, 3); •, (0, 4); ▲, (0, 5).

Figure 4. Ideal-gas heat-capacities for R-143a: ●; This work; ▲, Ichikawa *et al.*⁶; ○, This work; ◇, Yokozeki *et al.*⁸; □, Gillis¹⁰; +, Beckermann and Kohler¹⁵; ×, TRC¹⁶.

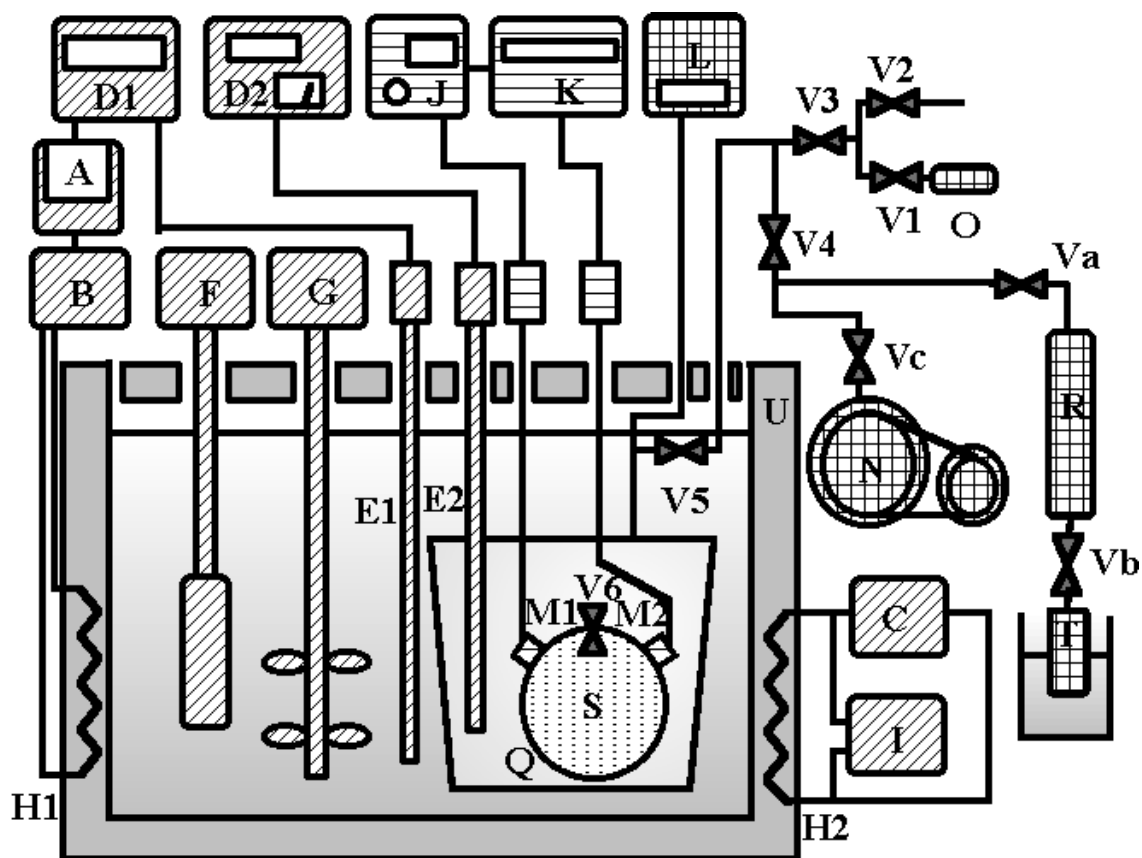


Figure 1. Experimental apparatus: (A) PID controller; (B) Thyristor regulator; (C) Transformer; (D1, D2) Thermometer bridges; (E1, E2) Platinum resistance thermometers; (F) Refrigeration units; (G) Stirrer; (H1, H2) Heaters; (I) Voltmeter; (J) Frequency synthesizer; (K) Lock-in amplifier; (L) Pressure gage; (M1)(M2) Transducers; (N) Vacuum pump; (O) Supply bottle; (Q) Pressure vessel; (R) Expansion bottle; (S) Spherical resonator; (T) Recovering bottle; (U) Thermostated bath; (V) Valves.

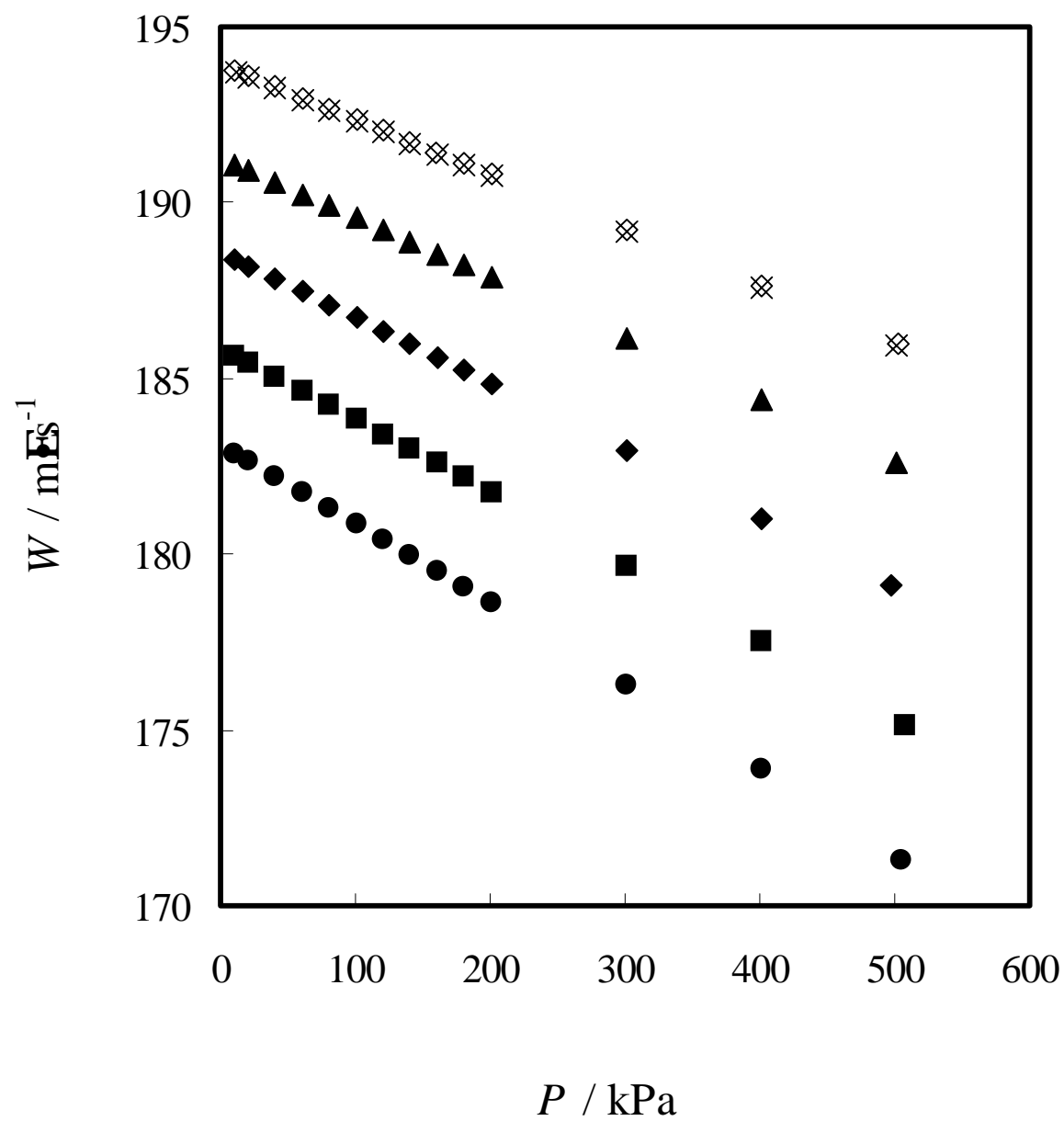


Figure 2. . Speed-of-sound measurements for R-143a: ●, 303K; ■, 313K; •, 323K; ▲, 333K; ◇, 343 K; ×, 343 K (previous sample).

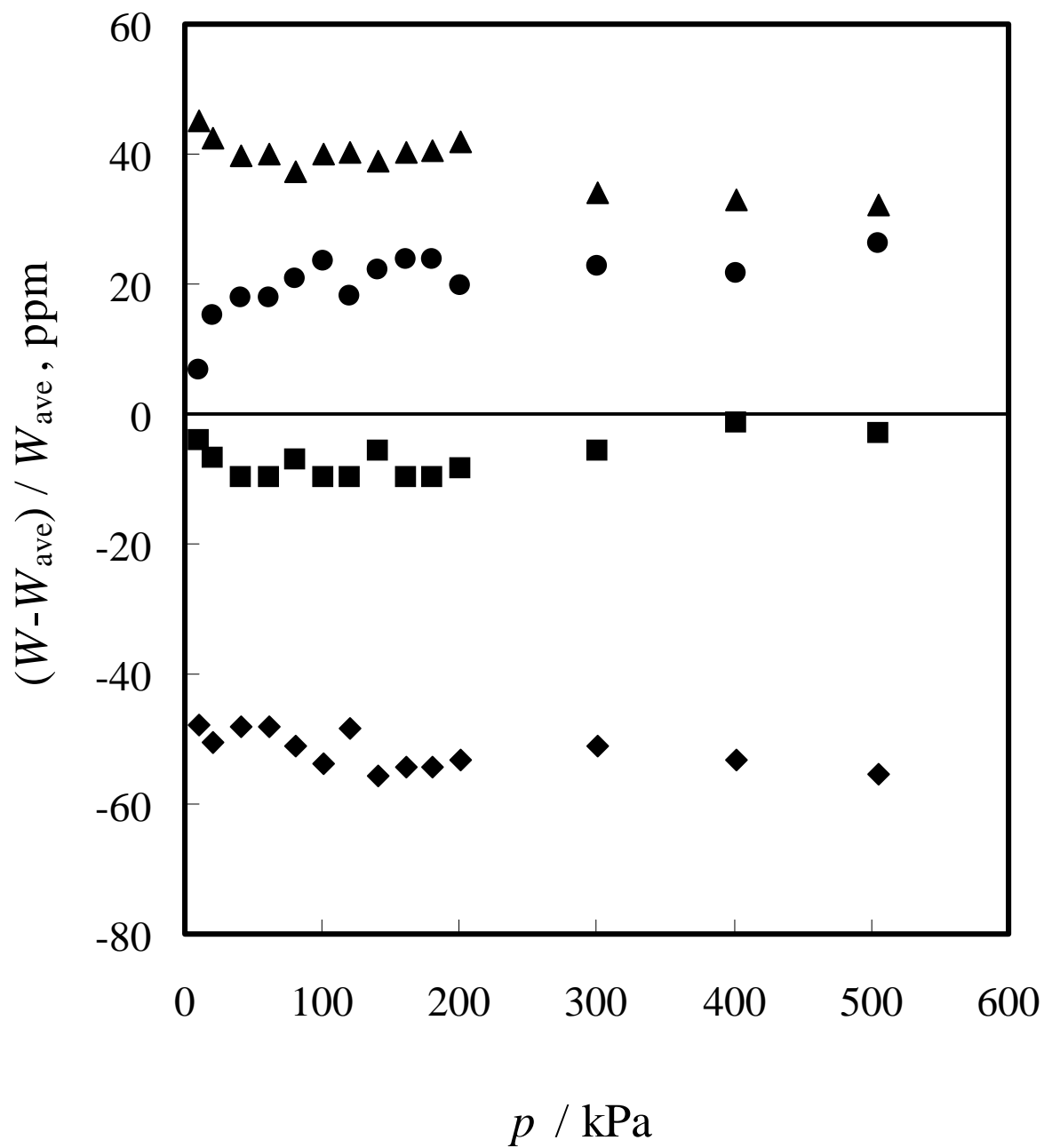


Figure 3 Difference among the speed-of-sound values at different modes: ●, (0, 2); ■, (0, 3); ♦, (0, 4); ▲, (0, 5).

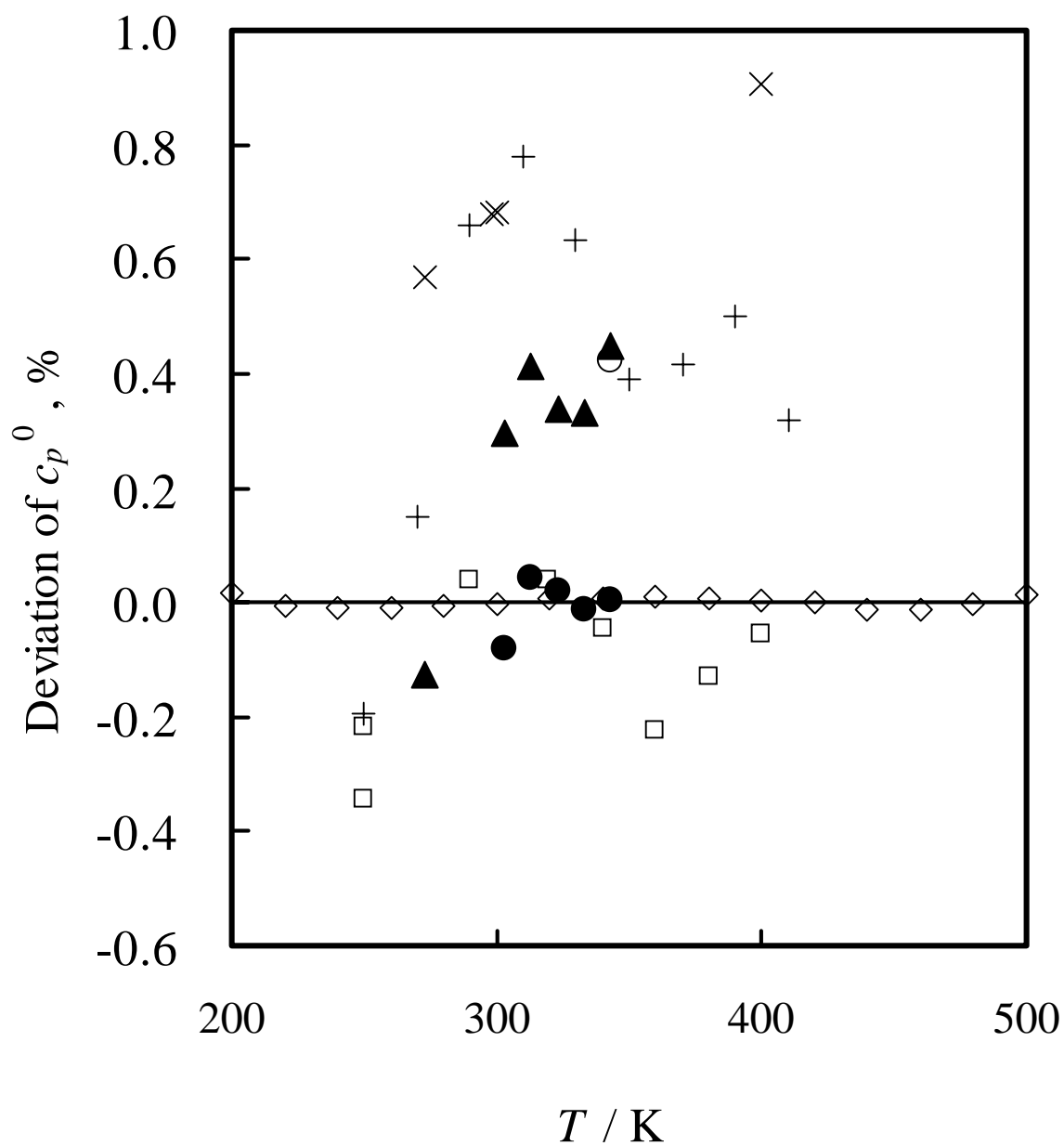


Figure 4. Ideal-gas heat-capacities for R-143a: ●; This work; ▲, Ichikawa *et al.*⁶; ○, This work; ◇, Yokozeki *et al.*⁸; □, Gillis¹⁰; +, Beckermann and Kohler¹⁵; ×, TRC¹⁶.